Available online at www.sciencedirect.com
ScienceDirect
Bioorganic & Medicinal Chemistry Letters 18 (2008) 2409–2413
Bioorganic & Medicinal Chemistry Letters

Fluoroolefins as amide bond mimics in dipeptidyl peptidase IV inhibitors

Scott D. Edmondson,[a,*] Lan Wei,[a] Jinyou Xu,[a] Jackie Shang,[b] Shiyao Xu,[b] Jianmei Pang,[b] Ashok Chaudhary,[c] Dennis C. Dean,[c] Huaibing He,[a] Barbara Leiting,[d] Kathryn A. Lyons,[a] Reshma A. Patel,[d] Sangita B. Patel,[e] Giovanna Scapin,[e] Joseph K. Wu,[d] Maria G. Beconi,[f] Nancy A. Thornberry[d] and Ann E. Weber[a]

[a]*Department of Medicinal Chemistry, Merck & Co. Inc., PO Box 2000, Rahway, NJ 07065, USA*
[b]*Preclinical Drug Metabolism and Pharmacokinetics, Merck & Co. Inc., PO Box 2000, Rahway, NJ 07065, USA*
[c]*DMPK Global Technologies, Merck & Co. Inc., PO Box 2000, Rahway, NJ 07065, USA*
[d]*Department of Metabolic Disorders, Merck & Co. Inc., PO Box 2000, Rahway, NJ 07065, USA*
[e]*Global Structural Biology, Merck & Co. Inc., PO Box 2000, Rahway, NJ 07065, USA*
[f]*Department of Drug Metabolism, Abbott Laboratories, 100 Abbott Park Road, Abbot Park, IL 60045, USA*

Received 30 January 2008; revised 18 February 2008; accepted 21 February 2008
Available online 26 February 2008

Abstract—The synthesis, selectivity, rat pharmacokinetic profile, and drug metabolism profiles of a series of potent fluoroolefin-derived DPP-4 inhibitors (**4**) are reported. A radiolabeled fluoroolefin **33** was shown to possess a high propensity to form reactive metabolites, thus revealing a potential liability for this class of DPP-4 inhibitors.

Since the approval of sitagliptin (**1**, Fig. 1) as a new treatment option for type 2 diabetics, inhibition of dipeptidyl peptidase IV (DPP-4) has become an established mechanism for the treatment of type 2 diabetes.[1] DPP-4 is responsible for the inactivation of glucagon-like peptide 1 (GLP-1) and glucose-dependent insulinotropic polypeptide (GIP), both of which enhance the secretion of insulin in a glucose-dependent manner. Additionally, GLP-1 has been shown to stimulate insulin biosynthesis, inhibit glucagon secretion, slow gastric emptying, reduce appetite, and stimulate the regeneration and differentiation of islet β-cells.[2,3] DPP-4 inhibition increases circulating GLP-1 and GIP levels in humans, which leads to decreased blood glucose levels, hemoglobin A_{1c} levels, and glucagon levels.[3,4] DPP-4 inhibitors offer a number of advantages over existing diabetes therapies including a lowered risk of hypoglycemia, the potential for weight loss, and the potential for the regeneration and differentiation of pancreatic β-cells.[5]

Previous reports from these laboratories described the optimization of a β-substituted phenylalanine derived class of DPP-4 inhibitors which culminated in the discovery of the potent and selective orally active DPP-4 inhibitor **2**.[6] Further work with β-substituted α-amino amides afforded a potent and selective oxadiazole class of DPP-4 inhibitors represented by **3**.[7] Surprisingly, X-

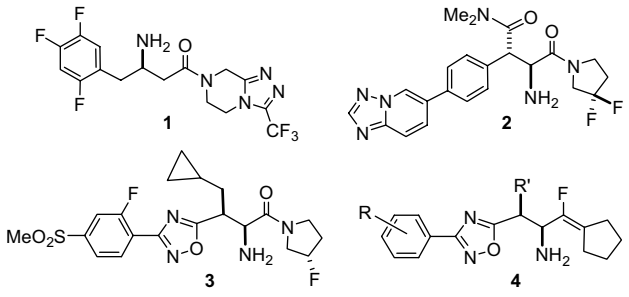

Figure 1. Potent and selective DPP-4 inhibitors, including sitagliptin (**1**), α-amino amides **2** and **3**, and fluoroolefins **4**.

Keywords: Fluoroolefin; DPP-4; Dipeptidyl peptidase IV; Oxadiazole; Amide bond mimic; Amide bond mimetic; Amide bond bioisostere; QPP; DPP-II.
* Corresponding author. Tel.: +1 732 594 0287; fax: +1 732 594 5350; e-mail: scott_edmondson@merck.com

0960-894X/$ - see front matter © 2008 Elsevier Ltd. All rights reserved.
doi:10.1016/j.bmcl.2008.02.050

ray crystallographic analysis of compounds from these structure classes revealed that **2** and **3** interact with distinct pockets of the DPP-4 binding site.

The identification of suitable amide bond bioisosteres is an active area in medicinal chemistry research.[8] Fluoroolefins represent one such class of bioisosteres that mimic amide bonds both geometrically and electronically,[9] and the successful incorporation of fluoroolefins as amide bond mimetics has been reported in multiple biologically relevant systems.[10] Welch and co-workers studied a series of fluoroolefin-derived DPP-4 inhibitors,[11] and more recently Van der Veken et al. also reported structure–activity relationships of a series of fluoroolefin-derived dipeptidyl peptidase inhibitors.[12] We sought to incorporate fluoroolefins as amide bond mimetics into the oxadiazole-derived DPP-4 inhibitors **3** in an effort to improve the selectivity and pharmacokinetic properties of this inhibitor class. This paper will describe the chiral synthesis and biological profile of a fluoroolefin class of DPP-4 inhibitors represented by the general structure **4**.

The synthesis of fluoroolefin DPP-4 inhibitors began with a Horner–Emmons reaction of triethyl 2-fluoro-2-phosphonoacetate with cyclopentanone (**5**) to form the somewhat volatile fluoroenoate, which was quickly reduced to afford allylic alcohol **6** (Scheme 1). Oxidation of **6** with Dess–Martin periodinane afforded the corresponding volatile aldehyde, which was immediately condensed with Ellman's (*R*) *tert*-butyl sulfinamide to give chiral imine **7**. Exposure of **7** to the titanium ester enolate of methyl acetate generated the desired *S*-amino stereocenter and subsequent protecting group manipulation produced the Boc protected amine **8**.[13] Alkylation of the potassium enolate of **9** with methyl iodide selectively afforded the *syn* ester diastereomer **9**,[7] which was hydrolyzed to give acid **10**. Condensation of **10** with the substituted benzamidoximes was followed by thermally induced cyclocondensation to furnish the desired oxadiazoles.[14] Deprotection of the Boc group then afforded the desired inhibitors **20**–**28**.[15]

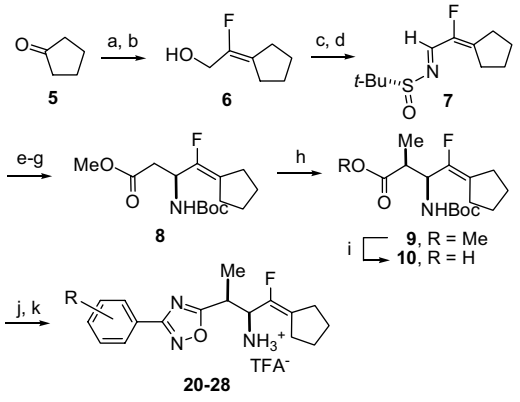

Scheme 1. Synthesis of DPP-4 inhibitors **20**–**28**. Reagents and conditions: (a) THF, NaH, $(EtO)_2POCHFCO_2Et$, rt; (b) DIBAl-H, Et_2O, −78 °C (79% yield, 2 steps); (c) Dess–Martin periodinane, CH_2Cl_2 (93% yield); (d) (*R*)-*t*-$BuSONH_2$, $Ti(OEt)_4$, THF, Δ (96% yield); (e) $MeCO_2Me$, LDA, $TiCl(Oi\text{-}Pr)_3$, THF; (f) MeOH, HCl; (g) THF, $NaHCO_3$ (aq), Boc_2O (75% yield, 3 steps); (h) KHMDS, MeI, THF, −78 °C (78% yield); (i) $LiOH_{(aq)}$, THF (86% yield); (j) EDC, $ArC(=NOH)NH_2$, CH_2Cl_2 then tol, dioxane, Δ; (k) TFA, CH_2Cl_2.

Ester **8** was also alkylated with allyl bromide to give a mixture of *syn*/*anti* diastereomeric α-allyl esters **11** (Scheme 2). Ester hydrolysis was followed by oxadiazole formation as above to afford **12**. The terminal olefin of **12** was next converted to an alcohol using the following three-step sequence: osmylation of the olefin to afford a diol, oxidative cleavage of the diol to give the acid, and reduction of the corresponding mixed anhydride to furnish the alcohol. Alternatively, **12** could be chemoselectively cyclopropanated by treatment with diazomethane under palladium catalysis.[16] Separation of the *syn*/*anti* diastereomers (*syn* was minor, Fig. 2) was followed by deprotection of the Boc groups to give alcohols **29**/**30** and cyclopropanes **31**/**32**.

A carbon-14 radiolabeled ethyl sulfone **33** was synthesized by treatment of methyl sulfone **13** with KHMDS and labeled methyl iodide (Scheme 3). Deprotection of the Boc group furnished ethyl sulfone **33**.

The potency and selectivity profiles of selected oxadiazole amides and fluoroolefins are reviewed in Table 1. Compounds were tested for inhibition of DPP-4 and selectivity over quiescent cell proline peptidase (QPP, DPP-II), prolyl endopeptidase (PEP), aminopeptidase P (APP), prolidase, DPP8, and DPP9.[17,18] The fluoroolefins generally displayed excellent (>1000-fold) selectivity for DPP-4 inhibition over the counterscreens,

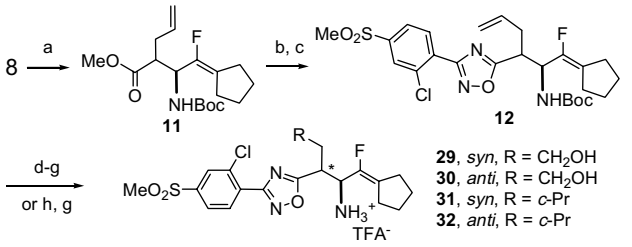

Scheme 2. Synthesis of DPP-4 inhibitors **29**–**32**. Reagents and conditions: (a) KHMDS, allyl bromide, THF, −78 °C; (b) $LiOH_{(aq)}$, THF (60% yield, 2 steps); (c) EDC, 2-Cl-4-$(MeSO_2)C_6H_3$–$C(=NOH)NH_2$, CH_2Cl_2 then tol, dioxane, Δ (33% yield); (d) OsO_4, THF, pyr (73% yield); (e) $NaIO_4$, $KMnO_4$, THF, H_2O; (f) $ClCO_2i\text{-}Pr$, THF then $NaBH_4$, MeOH, separate diastereomers (43% yield, 2 steps; *syn*/*anti* = 1:2 ratio); (g) TFA, CH_2Cl_2; (h) CH_2N_2, $Pd(OAc)_2$, Et_2O, separate diastereomers (55% yield, *syn*/*anti* = 1:1.5 ratio).

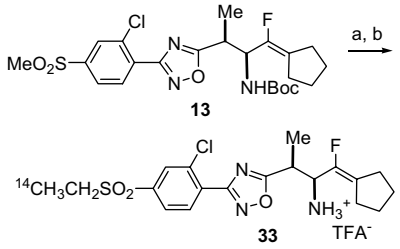

Scheme 3. Synthesis of radiolabelled ethyl sulfone **33**. Reagents: (a) KHMDS, $^{14}CH_3I$, THF; (b) TFA, CH_2Cl_2.

including DPP8 and DPP9.[19] They were less selective over QPP, however, thus only QPP data are presented for comparison. Although the dichlorophenyl amide **14** was more potent than the fluoroolefin counterpart **20**, the phenyl methyl sulfone amides such as **15** and **16** (DPP-4 IC_{50}'s = 122 nM and 17 nM, respectively) were somewhat less potent than the corresponding fluoroolefins **23** and **26** (DPP-4 IC_{50}'s = 90 nM and 7.5 nM, respectively). Similar to previously reported data in the oxadiazole series,[7] the addition of a fluorine atom to the pyrrolidine ring in the amides resulted in ~2.4-fold loss of potency at DPP-4 (e.g., **16** vs **17**). Thus, while structurally similar fluoroolefins **29** and **31** were 22-fold and 62-fold more potent at DPP-4 compared to **18** and **19**, some of the reduced potency observed with **18** and **19** is likely due to the presence of a fluorine atom on the pyrrolidine ring in this series of inhibitors.

Not surprisingly, potency for QPP inhibition also increased substantially in the fluoroolefin series relative to the amides.[12b] In contrast to previous reports, however, many of the fluoroolefins in Table 1 possess excellent potency for DPP-4 inhibition. To better understand the structural features of these fluoroolefins that afford potent DPP-4 inhibition, X-ray crystal structures of **3** and **31** bound to DPP-4 were obtained.

Co-crystallization of **3** (green) and **31** (yellow) with DPP-4 shows that the major interactions of these inhibitors with DPP-4 are similar (Fig. 2).[20] Additionally, the

Table 1. Selected oxadiazole-derived DPP-4 inhibitors with amide bonds and with fluoroolefins

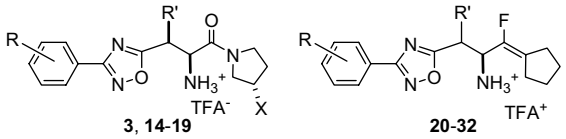

Compound	R	R′	X	IC_{50} (μM)	
				DPP-4	QPP
3	2-F, 4-SO_2Me	CH_2cPr	F	0.019	18
14	2,4-diCl	Me	H	0.203	1.4
15	4-SO_2Me	Me	H	0.122	15
16	2-Cl, 4-SO_2Me	Me	H	0.017	6.4
17	2-Cl, 4-SO_2Me	Me	F	0.040	3.5
18	2-Cl, 4-SO_2Me	$(CH_2)_2$OH	F	0.070	45
19	2-Cl, 4-SO_2Me	CH_2cPr	F	0.013	17
20	2,4-diCl	Me	—	1.165	0.25
21	2-Cl, 4-CF_3	Me	—	0.525	1.66
22	2-Cl, 4-Br	Me	—	0.645	0.14
23	4-SO_2Me	Me	—	0.090	3.91
24	4-SO_2CF_3	Me	—	1.490	3.44
25	2-Cl, 4-$NHSO_2$Me	Me	—	0.057	0.33
26	2-Cl, 4-SO_2Me	Me	—	0.0075	0.33
27	2-Cl, 4-SO_2Et	Me	—	0.050	0.42
28	2-Cl, 4-SO_2Me	H	—	0.021	0.46
29[a]	2-Cl, 4-SO_2Me	$(CH_2)_2$OH	—	0.0032	1.16
30[a]	2-Cl, 4-SO_2Me	$(CH_2)_2$OH	—	0.093	1.40
31[a]	2-Cl, 4-SO_2Me	CH_2cPr	—	0.00021	0.13
32[a]	2-Cl, 4-SO_2Me	CH_2cPr	—	0.012	0.21

[a] **29** and **31** are *syn* disastereomers, **30** and **32** are *anti* diastereomers.

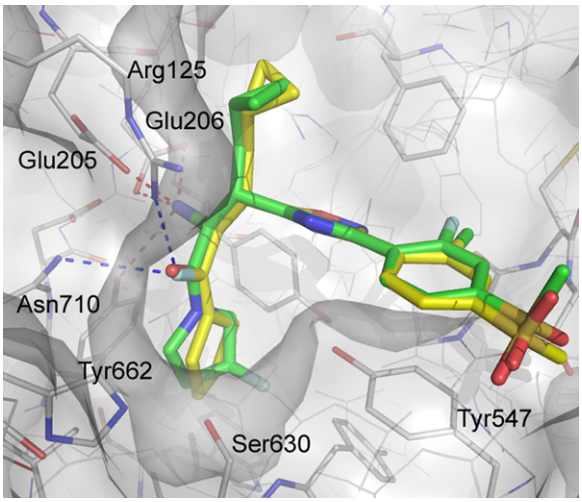

Figure 2. X-ray crystal structures of amide **3** (green) and fluoroolefin **31** (yellow) bound to DPP-4.[20] Interactions of **3** and **31** with DPP-4 are shown in blue dotted lines. All water molecules and their hydrogen bond networks have been omitted for clarity.

X-ray structure confirms the *syn* stereochemical assignment of potent DPP-4 inhibitor **31**. Consistent with the previously reported X-ray structure of compound **15**,[7] the phenyl ring of **3** appears to stack against the side chain of Tyr547. Although the cyclopropyl groups are oriented into a hydrophobic pocket, they do not reach far enough into this pocket to interact with Arg358, which has been shown to be an important DPP-4 binding residue with other selective inhibitors such as **2**.[6] Not surprisingly, the fluoroolefin functionality of **31** forces the cyclopentane ring into a coplanar orientation with the double bond. In contrast, the pyrrolidide ring of **3** appears to be bent slightly out of the plane of the amide pi-system. Consequently, the cyclopentane ring of **31** and the pyrrolidine ring of **3** adopt slightly different orientations in the DPP-4 binding pocket. The fluorine atom in **31** aligns well with the amide carbonyl oxygen of **3** and each of these atoms forms two hydrogen bond interactions with Asn710 and Glu206 in their respective X-ray crystal structures.

Inhibitors that possessed superior potency and selectivity profiles were evaluated for their rat pharmacokinetic properties (Table 2). Activity at hERG was also measured in order to assess potential cardiovascular liabilities.[21] Selectivity over hERG was excellent for the three fluoroolefins evaluated, but the oral bioavailabilities of alcohol **29** ($F = 4\%$) and cyclopropane **31**

Table 2. Pharmacokinetic properties of selected DPP-4 inhibitors in the rat (1/2 mg/kg iv/po) and hERG binding

Compound	Clp (mL/min/kg)	$t_{1/2}$ (h)	F (%)	hERG IC_{50} (μM)
16	6	0.86	27	37
26	20	2.0[a]	62	19
29	51	1.6	4	47
31	54	1.5	1	7.1

[a] Value for mean residence time (MRT) is reported since $t_{1/2}$ could not be calculated due to secondary peaks in the plasma concentration time profile.

Table 3. Rat hepatocyte and rat liver microsomal stability of amide **16** and fluoroolefin **26**

Compound	% Parent remaining at 60 min	
	RLM[a] + NADPH	Rat hepatocytes
16	56%	88%
26	<LOQ[b]	3%

[a] RLM, rat liver microsomes.
[b] LOQ, limits of quantitation.

($F = 1\%$) were too low to merit further profiling. In contrast, methyl analog **26** displayed improved oral bioavailability ($F = 62\%$) relative to **29** and **31** and the corresponding amide derivative **16** ($F = 27\%$). On the other hand, **26** also exhibited increased clearance relative to amide **16**.

In order to better understand the difference in rat intrinsic clearance between **16** and **26**, each compound was incubated with rat hepatocytes and rat liver microsomes and the percentage parent remaining was measured at 60 min (Table 3). Fluoroolefin **26** was significantly less stable than amide **16** in rat liver microsome and hepatocyte incubations, and the metabolism of **26** in liver microsomes was NADPH-dependent. Mass spectrometric analyses of the rat liver microsome and hepatocyte incubations of **16** revealed a predominance of oxidative metabolites formed on the pyrrolidine ring.[22] In contrast, major metabolites identified from fluoroolefin **26** were oxidized at the cyclopentanyl fluoroolefin moiety. Moreover, multiple glutathione adducts were detected in the incubations with fluoroolefin **26**, indicating a potential propensity for this compound to form reactive metabolites.

To further assess the potential for bioactivation of the fluoroolefin series of DPP-4 inhibitors, a ^{14}C-radiolabeled ethyl sulfone derivative **33** was synthesized and evaluated in the in vitro covalent binding assay in rat and human liver microsomes.[22,23] Compound **33** displayed a high potential for metabolic activation in both species, with levels of irreversible binding of 662 pmol/mg protein and 287 pmol/mg protein in rat and human liver microsomes, respectively. The irreversible binding of **33** was NADPH-dependent and was attenuated in the presence of glutathione in the incubations, indicating that chemically reactive intermediates were formed and trapped by the nucleophilic thiol of glutathione. High levels of irreversible binding can indicate a potential propensity for a drug to form covalent linkages with proteins or other large biomolecules in vivo. The resulting haptens can then lead to idiosyncratic drug reactions.[24] Consequently, further evaluation of this potent and selective fluoroolefin series of DPP-4 inhibitors was discontinued.

In conclusion, a new series of potent and selective DPP-4 inhibitors were described in which a fluoroolefin moiety replaced a central amide bond. Comparison of an X-ray crystal structure of the potent fluoroolefin **31** with the structurally related amide **3** shows that the fluoroolefin moiety behaves as an effective amide bioisostere in the DPP-4 binding pocket. Evaluation of a series of fluoroolefins in rat pharmacokinetics studies revealed that **26** shows improved oral bioavailability but higher intrinsic clearance compared to the structurally related amide derivative **16**. Incubation of the radiolabeled fluoroolefin **33** with rat and human liver microsomes showed that this compound has a high propensity to form reactive metabolites that can irreversibly bind to biomolecules. Consequently, the potential liabilities associated with the high propensity for bioactivation of these fluoroolefins led to discontinuation of the evaluation of this class of potent and selective DPP-4 inhibitors.

Acknowledgments

The authors thank I. Capodanno, M. Donnelly, J.E. Fenyk-Melody, J. Hausamann, C. Nunes, X. Shen, J. Strauss, K. Vakerich, Z. Yao for dosing the animals used in pharmacokinetic experiments.

Supplementary data

Supplementary data associated with this article can be found, in the online version, at doi:10.1016/j.bmcl.2008.02.050.

References and notes

1. (a) Thornberry, N. A.; Weber, A. E. *Curr. Top. Med. Chem.* **2007**, *7*, 557; (b) Edmondson, S. D.; Kim, D. Selective dipeptidyl peptidase IV inhibitors for the treatment of type 2 diabetes: the discovery of JANUVIA™ (sitagliptin). In *Methods and Principles in Medicinal Chemistry, Antitargets* Vaz, R. J., Klabunde, T. Eds.; Wiley-VCH, 2008; Vol. 38, 401–422; (c) Herman, G. A.; Stein, P. P.; Thornberry, N. A.; Wagner, J. A. *Clin. Pharm. Ther.* **2007**, *81*, 761.
2. For lead DPP-4 references, see: (a) Idris, I.; Donnelly, R. *Diab. Obes. Metab.* **2007**, *9*, 153; (b) von Geldern, T. W.; Trevillyan, J. M. *Drug Dev. Res.* **2006**, *67*, 627; (c) Augustyns, K.; Van der Veken, P.; Haemers, A. *Expert Opin. Ther. Pat.* **2005**, *15*, 1387.
3. For lead GLP-1 references, see: (a) Holst, J. J. *Physiol. Rev.* **2007**, *87*, 1409; (b) Drucker, D. J. *Cell Metab.* **2006**, *3*, 153; (c) Drucker, D. J.; Nauck, M. A. *The Lancet* **2006**, *368*, 1696.
4. During, M. J.; Cao, L.; Zuzga, D. S.; Francis, J. S.; Fitzsimons, H. L.; Jiao, X.; Bland, R. J.; Klugmann, M.; Banks, W. A.; Drucker, D. J.; Haile, C. N. *Nat. Med.* **2003**, *9*, 1173.
5. (a) Meece, J. *Curr. Med. Res. Opin.* **2007**, *23*, 933; (b) Ahren, B.; Landin-Olsson, M.; Jansson, P.-A.; Svensson, M.; Holmes, D.; Schweizer, A. *J. Clin. Endocrin. Metab.* **2004**, *89*, 2078.
6. Edmondson, S. D.; Mastracchio, A.; Mathvink, R. J.; He, J.; Harper, B.; Park, J.-J.; Beconi, M.; Di Salvo, J.; Eiermann, G. J.; He, H.; Leiting, B.; Leone, J. F.; Levorse, D. A.; Lyons, K.; Patel, R. A.; Patel, S. B.; Petrov, A.; Scapin, G.; Shang, J.; Sinha Roy, R.; Smith, A.; Wu, J. K.; Xu, S.; Zhu, B.; Thornberry, N. A.; Weber, A. E. *J. Med. Chem.* **2006**, *49*, 3614.

7. Xu, J.; Wei, L.; Mathvink, R. J.; Edmondson, S. D.; Eiermann, G. J.; He, H.; Leone, J. F.; Leiting, B.; Lyons, K. A.; Marsilio, F.; Patel, R. A.; Patel, S. B.; Petrov, A.; Scapin, G.; Wu, J. K.; Thornerry, N. A.; Weber, A. E. *Bioorg. Med. Chem. Lett.* **2006**, *16*, 5373.
8. For lead references, see: (a) Legeay, J. C.; Eynde, J. C. V.; Bazureau, J. P. *Tetrahedron Lett.* **2007**, *48*, 1063; (b) Coburn, C. A.; Stachel, S. J.; Jones, K. G.; Steele, T. G.; Rush, D. M.; DiMuzio, J.; Pietrack, B. L.; Lai, M.-T.; Huang, Q.; Lineberger, J.; Jin, L.; Munshi, S.; Holloway, M. K.; Espeseth, A.; Simon, A.; Hazuda, D.; Graham, S. L.; Vacca, J. P. *Bioorg. Med. Chem. Lett.* **2006**, *16*, 3635; (c) Black, W. C.; Bayly, C. I.; Davis, D. E.; Desmarais, S.; Falgueyret, J.-P.; Leger, S.; Li, C. S.; Masse, F.; McKay, D. J.; Palmer, J. T.; Percival, M. D.; Robichaud, J.; Tsou, N.; Zamboni, R. *Bioorg. Med. Chem. Lett.* **2005**, *15*, 4741; (d) Venkatesan, N.; Kim, B. H. *Curr. Med. Chem.* **2002**, *9*, 2243.
9. (a) Abraham, R. J.; Ellison, S. L. R.; Schonholzer, P.; Thomas, W. A. *Tetrahedron* **1986**, *42*, 2101; (b) Allmendinger, T.; Furet, P.; Hungerbuhler, E. *Tetrahedron Lett.* **1990**, *31*, 7297; (c) Welch, J. T.; Allmendenger, T. In *Peptidomimetic Protocols*; Kazmierski, W. M., Ed.; Humana Press: New Jersey, 1999; pp 375–384.
10. (a) Allmendenger, T.; Felder, E.; Hungerbuhler, E. *Tetrahedron Lett.* **1990**, *31*, 7301; (b) Boros, L.; De Corte, B.; Gimi, R. H.; Welch, J. T.; Wu, Y.; Handschumacher, R. E. *Tetrahedron Lett.* **1994**, *35*, 6033; (c) Bartlett, P. A.; Otake, A. *J. Org. Chem.* **1995**, *60*, 3107; (d) Niida, A.; Tomita, K.; Mizumoto, M.; Tanigaki, H.; Terada, T.; Oishi, S.; Otaka, A.; Inui, K.; Fujii, N. *Org. Lett.* **2006**, *8*, 613.
11. (a) Welch, J. T.; Lin, J. *Tetrahedron* **1996**, *52*, 291; (b) Lin, J.; Toscano, P. J.; Welch, J. T. *Proc. Natl. Acad. Sci. U.S.A.* **1998**, *95*, 14020; (c) Zhao, K.; Lim, D. S.; Funaki, T.; Welch, J. T. *Bioorg. Med. Chem. Lett.* **2003**, *11*, 207.
12. (a) Van der Veken, P.; Kertesz, I.; Senten, K.; Haemers, A.; Augustyns, K. *Tetrahedron Lett.* **2003**, *44*, 6231; (b) Van der Veken, P.; Senten, K.; Kertesz, I.; De Meester, I.; Lambeir, A.-M.; Maes, M.-B.; Scharpe, S.; Haemers, A.; Augustyns, K. *J. Med. Chem.* **2005**, *48*, 1768.
13. Tang, T. P.; Ellman, J. A. *J. Org. Chem.* **2002**, *67*, 7819.
14. Liang, G.-B.; Feng, D. D. *Tetrahedron Lett.* **1996**, *37*, 6627.
15. All final compounds were characterized by ^{1}H NMR and LC–MS.
16. Suda, M. *Synthesis* **1981**, *9*, 714.
17. IC_{50} determinations for DPP-4 and QPP were carried out as described in: Leiting, B.; Pryor, K. D.; Wu, J. K.; Marsilio, F.; Patel, R. A.; Craik, C. S.; Ellman, J. A.; Cummings, R. T.; Thornberry, N. A. *Biochem. J.* **2003**, *371*, 525.
18. All DPP-4 IC_{50}'s are an average of $n \geqslant 2$, with standard deviations less than 75% of the average.
19. For a discussion of the relevance of selectivity over DPP8 and DPP9, see: Lankas, G. R.; Leiting, B.; Sinha Roy, R.; Eiermann, G. J.; Beconi, M. G.; Biftu, T.; Chan, C.-C.; Edmondson, S.; Feeney, W. P.; He, H.; Ippolito, D. E.; Kim, D.; Lyons, K. A.; Ok, H. O.; Patel, R. A.; Petrov, A. N.; Pryor, K. A.; Qian, X.; Reigle, L.; Woods, A.; Wu, J. K.; Zaller, D.; Zhang, X.; Zhu, L.; Weber, A. E.; Thornberry, N. A. *Diabetes* **2005**, *54*, 2988.
20. The atomic coordinates for the X-ray structures of DPP-4 in complex with **3** and **31** have been deposited into the RCSB protein data bank under RCSB ID codes rcsb046315 and rscb046317, and under PDB ID codes 3C43 and 3C45, respectively.
21. IC_{50} determinations for hERG was carried out as described in: Friesen, R. W.; Ducharme, Y.; Ball, R. G.; Blouin, M.; Boulet, L.; Cote, B.; Frenette, R.; Girard, M.; Guay, D.; Huang, Z.; Jones, T. R.; Laliberte, F.; Lynch, J. J.; Mancini, J.; Martins, E.; Masson, P.; Muise, E.; Pon, D. J.; Siegel, P. K. S.; Styhler, A.; Tsou, N. N.; Turner, M. J.; Young, R. N.; Girard, Y. *J. Med. Chem.* **2003**, *46*, 2017.
22. For related work done to identify metabolites on fluoropyrrolidine-derived DPP-4 inhibitors, see: Xu, S.; Zhu, B.; Teffera, Y.; Pan, D. E.; Caldwell, C. G.; Doss, G.; Stearns, R. A.; Evans, D. C.; Beconi, M. G. *Drug Metab. Dispos.* **2005**, *33*, 121.
23. Evans, D. C.; Watt, A. P.; Nicoll-Griffith, D. A.; Baillie, T. A. *Chem. Res. Toxicol.* **2004**, *17*, 3.
24. Uetrecht, J. P. *Chem. Res. Toxicol.* **1999**, *12*, 387.